Journal of Solid State Chemistry **166,** 442–448 (2002)
doi:10.1006/jssc.2002.9627

New Molybdenyl Iodates: Hydrothermal Preparation and Structures of Molecular $K_2MoO_2(IO_3)_4$ and Two-Dimensional β-$KMoO_3(IO_3)$

Richard E. Sykora, Daniel M. Wells, and Thomas E. Albrecht-Schmitt[1,2]

Department of Chemistry, 179 Chemistry Building, Auburn University, Auburn, Alabama 36849

Received February 19, 2002; in revised form April 8, 2002; accepted April 19, 2002

Two new molybdenyl iodates, $K_2MoO_2(IO_3)_4$ (1) and β-$KMoO_3(IO_3)$ (2), have been prepared from the reactions of MoO_3 with KIO_4 and NH_4Cl at 180°C in aqueous media. The structure of 1 consists of molecular $[MoO_2(IO_3)_4]^{2-}$ anions separated by K^+ cations. The Mo(VI) centers are ligated by two *cis*-oxo ligands and four monodentate iodate anions. Both terminal and bridging oxygen atoms of the iodate anions form long ionic contacts with the K^+ cations. β-$KMoO_3(IO_3)$ (2) displays a two-dimensional layered structure constructed from $^2_\infty[(MoO_3(IO_3))]^{1-}$ anionic sheets separated by K^+ cations. These sheets are built from one-dimensional chains formed from corner-sharing MoO_6 octahedra that run along the *b*-axis that are linked together through bridging iodate groups. K^+ cations separate the layers from one another and form long contacts with oxygen atoms from both the iodate anions and molybdenyl moieties. Crystallographic data: 1, monoclinic, space group $C2/c$, $a = 12.8973(9)$ Å, $b = 6.0587(4)$ Å, $c = 17.694(1)$ Å, $\beta = 102.451(1)^\circ$, $Z = 4$, Mo$K\alpha$, $\lambda = 0.71073$, $R(F) = 2.64\%$ for 97 parameters with 1584 reflections with $I > 2\sigma(I)$; 2, monoclinic, space group $P2_1/n$, $a = 7.4999(6)$ Å, $b = 7.4737(6)$ Å, $c = 10.5269(8)$ Å, $\beta = 109.023(1)^\circ$, $Z = 4$, Mo$K\alpha$, $\lambda = 0.71073$, $R(F) = 2.73\%$ for 83 parameters with 1334 reflections with $I > 2\sigma(I)$. © 2002 Elsevier Science (USA)

INTRODUCTION

The preparation of molybdenum iodates dates to the late 19th century with several contributions by Blomstrand (1), Chrétien (2), and Rosenheim and Liebknecht (3). The exact nature of the compounds reported in these papers is difficult to ascertain because this work pre-dates the introduction of spectroscopic techniques and the discovery of X-ray diffraction. However, detailed elemental analyses and estimates of stoichiometry do exist. Renewed interest in transition metal iodates did not resurface until the early 1970s. At this time, it was recognized that anions containing stereochemically active lone pairs of electrons had a propensity for forming low-dimensional structures that were often also non-centrosymmetric. Given the potential usefulness of these compounds as non-linear optical, ferroelectric, pyroelectric, and piezoelectric materials, a large number of first-row transition metal and lanthanide iodates were prepared and characterized by X-ray diffraction techniques and extensive physical property measurements (4–13).

There are a number of reasons for reinvestigating high-valent early transition metal iodate chemistry. First, the structures and properties of the compounds reported in the 1890s are essentially unknown. Second, the structural versatility of early transition metals allows for a plethora of compounds to be isolated through the use of structure-directing counter-cations and variations in synthetic methodology. Finally, the optical properties of these compounds may prove to be quite interesting because in addition to the presence of a stereochemically active lone pair of electrons on iodine (14), there is a great likelihood of distortions away from octahedral symmetry around Mo(VI) owing to second-order Jahn–Teller effects (15–23).

One of the reasons that *d*- and *f*-block iodates can show such dramatic variations in structural architectures and dimensionality is that the iodate anion has three oxo groups that are each capable of coordinating up to two metal centers. As a consequence of this, it is difficult to predict the crystal chemistry of these compounds. For instance, the iodate anion can simply act as a monodentate Lewis base as observed in molecular $K[CrO_3(IO_3)]$ (24). More commonly, the iodate anion bridges between two metal centers as illustrated by $VO_2IO_3 \cdot 2H_2O$ (25) and $Ce(IO_3)_4 \cdot H_2O$ (26). However, all three oxo groups can be used to bridge three metal centers, which was observed in $Sm(IO_3)_3$ (10, 12). A rare mode of coordination also exists whereby a single iodate anion can chelate one metal and through a μ_3-oxo atom simultaneously bind a second metal

---

[1] To whom correspondence should be addressed. Fax: (334) 844-6959. E-mail: albreth@auburn.edu.

[2] Tables of anisotropic displacement parameters and structure factors for **1** and **2** are available upon request.

0022-4596/02 $35.00

center. This form of ligation is responsible for the formation of one-dimensional chains in $UO_2(IO_3)_2$ (27).

We have recently shown that alkali metal cations have structure-directing influences on Mo(VI) iodates (28). In this previous study, we demonstrated that when the largest members of the alkali metal group, Rb^+ and Cs^+, were used as counter-cations that three-dimensional, polar solids with the formula $A\mathrm{MoO_3(IO_3)}$ (A = Rb, Cs) could be isolated. However, the K^+ analog of these compounds, α-$KMoO_3(IO_3)$, is both layered and centrosymmetric. The former compounds crystallize in the polar space group $Pna2_1$, and show large second-harmonic generation (SHG) responses of 400 × α-quartz. In addition, these materials can be prepared in high yield and are both thermally and hydrolytically stable.

Herein, we report the continuation of these studies on the hydrothermal syntheses, structures, and physical properties of two new potassium molybdenyl iodates, $K_2MoO_2(IO_3)_4$ (**1**) and β-$KMoO_3(IO_3)$ (**2**). These compounds illustrate the complexity of the MoO_3:KIO_4:NH_4Cl compositional space and demonstrate how subtle changes in stoichiometry and reaction conditions can lead to dramatic changes in product composition.

EXPERIMENTAL

Syntheses

MoO_3 (99.95%, Alfa-Aesar), KIO_4 (99.9%, Fisher), and NH_4Cl (99.9%, Fisher) were used as received. Distilled and millipore-filtered water with a resistance of 18.2 MΩ was used in all reactions. All reactions were run in Parr 4749 23-mL autoclaves with PTFE liners. SEM/EDX analyses were performed using a JEOL 840/Link Isis instrument. K and Mo percentages were calibrated against standards. Typical results are within 4% of the ratios determined by single-crystal X-ray diffraction. IR spectra were collected on a Nicolet 5PC FT-IR spectrometer from KBr pellets.

$K_2MoO_2(IO_3)_4$ (1)

MoO_3 (105 mg, 0.731 mmol), KIO_4 (336 mg, 1.46 mmol), and NH_4Cl (59 mg, 1.10 mmol) were loaded in a 23-mL PTFE-lined autoclave. Water (1 mL) was then added to the solids resulting in an initial pH of 2.9. The autoclave was sealed and placed in a box furnace and then heated to 180°C, where the reaction occurred under autogenously generated pressure. After 72 h the furnace was cooled at 9°C/h to 23°C. The product mixture included clusters of colorless rods and colorless rhombohedra covered by a dark yellow liquid. The mother liquor of pH 0.30 was decanted from the crystals, which were then washed with methanol and allowed to dry. The rhombohedra of **1** could manually be separated from the colorless rods of **2** to afford a yield of 147 mg (45% based on Mo). EDX analysis for $K_2MoO_2(IO_3)_4$ provided a K:Mo:I ratio of 2:1:4. IR (KBr, cm^{-1}): 926 (s), 882 (s), 830 (w, sh), 818 (s), 760 (s), 741 (s), 713 (s), 635 (s, br), 567 (m, br), 495 (s), 452 (w, sh), 411 (s).

β-$KMoO_3(IO_3)$ (2)

MoO_3 (168 mg, 1.17 mmol), KIO_4 (269 mg, 1.17 mmol), and NH_4Cl (63 mg, 1.17 mmol) were loaded in a 23-mL PTFE-lined autoclave. Water (1 mL) was then added to the solids resulting in an initial pH of 2.9. The autoclave was sealed and placed in a box furnace that was then heated to 180°C, where the reaction occurred under autogenously generated pressure. After 72 h, the furnace was cooled at 9°C/h to 23°C. The product consisted of clusters of colorless rods covered by a dark yellow liquid. The mother liquor of pH 0.43 was decanted from the crystals, which were then washed with methanol and allowed to dry. The colorless rods of **2** afforded a yield of 182 mg (43% based on Mo). EDX analysis for β-$KMoO_3(IO_3)$ provided a K:Mo:I ratio of 1:1:1. IR (KBr, cm^{-1}): 931 (s), 917 (s, sh), 878 (s), 839 (s), 817 (s), 669 (s, br).

Crystallographic Studies

Single crystals of **1** and **2** with the dimensions of 0.144 × 0.184 × 0.204 mm and 0.036 × 0.074 × 0.136 mm, respectively, were mounted on glass fibers and aligned on a Bruker SMART APEX CCD diffractometer. For each crystal, intensity measurements were performed using graphite monochromatic Mo$K\alpha$ radiation from a sealed tube and a monocapillary collimator. SMART was used for a preliminary determination of the cell constants and data collection control. The intensities of reflections of a sphere were collected by a combination of three sets of exposures (frames). Each set had a different φ angle for the crystal and each exposure covered a range of 0.3° in ω. A total of 1800 frames were collected with an exposure time per frame of 10 s for **1** and 30 s for **2**.

The determination of integral intensities and global cell refinement were performed with the Bruker SAINT (v 6.02) software package using a narrow-frame integration algorithm. A semi-empirical absorption correction was applied based on the intensities of symmetry-related reflections measured at different angular settings using SADABS (29). The program suite SHELXTL (v 5.1) was used for space group determination (XPREP), direct methods structure solutions (XS), and structure refinement (XL) (30). The final refinement included anisotropic displacement parameters for all atoms. The data collection and structure solution for $K_2MoO_2(IO_3)_4$ (**1**) were straightforward. However, β-$KMoO_3(IO_3)$ (**2**) proved to be more problematic as a large number of crystals were twinned. After trying multiple crystals, a very small needle from a low-yield reaction proved to be single. During initial cell refinement with SMART, the Bravais option suggested a primitive orthorhombic cell as well as the correct primitive monoclinic cell. The systematic absences, however, were not consistent with an *mmm* Laue group. After the structure was solved and refined in the monoclinic setting $P2_1/n$, the ADDSYMM and NEWSYMM programs of Platon (31) were employed to test for missed symmetry. None was suggested. Some crystallographic details are listed in Tables 1–3. Additional details of anisotropic displacement parameters and structure factors for **1** and **2** are available upon request.

RESULTS AND DISCUSSION

Syntheses

The reactions of MoO_3, KIO_4, and NH_4Cl have led to the production of two new potassium molybdenyl iodates, $K_2MoO_2(IO_3)_4$ (**1**) and β-$KMoO_3(IO_3)$ (**2**). Compound **1** has only been produced along with **2**, despite carrying out a number of reactions varying reactant stoichiometries and pH in hope of producing **1** in pure form. The changes in reaction stoichiometry have a substantial effect on the isolated yields of **1** and **2**. The ratio of β-$KMoO_3(IO_3)$:$K_2MoO_2(IO_3)_4$ can be increased by holding the ratio of MoO_3 and KIO_4 constant at a 1:2 ratio and increasing the number of equivalents of NH_4Cl. The highest percent yield of **1** has been observed at 45%. β-$KMoO_3(IO_3)$ can be prepared as the sole product of the reaction of MoO_3, KIO_4, and NH_4Cl by using a 1:1:1 ratio. However, the large crystals recovered from these reactions are severely twinned, and the isolated yield is lower in comparison to reactions producing a mixture of products that can be manually separated.

The reactions used to prepare **1** and **2** are not stoichiometry driven alone as both of these new compounds have only been produced when NH_4Cl is present in the reactions. The α-$KMoO_3(IO_3)$ phase can be produced in high yield along with KIO_3 with a 1:2 molar ratio of MoO_3:KIO_4 in the absence of NH_4Cl as previously reported (28). The same ratio of MoO_3 and KIO_4 with the addition of NH_4Cl, however, has the effect of yielding **1** and **2** in varying amounts depending on the quantity of NH_4Cl added. Evidently, the lowered pH influences the reaction products, since neither NH_4^+ nor Cl^- ions are incorporated into **1** or **2** as evidenced by CHN and EDX analyses. The observation of dark yellow mother liquors

TABLE 1
Crystallographic Data for $K_2MoO_2(IO_3)_4$ (1) and β-$KMoO_3(IO_3)$ (2)

Formula	$K_2MoO_2(IO_3)_4$	β-$KMoO_3(IO_3)$
Formula mass (amu)	905.74	357.94
Color and habit	Colorless, rhombohedron	Colorless, octagonal plate
Space group	$C2/c$ (no.15)	$P2_1/n$ (no. 14)
a (Å)	12.8973(9)	7.4999(6)
b (Å)	6.0587(4)	7.4737(6)
c (Å)	17.694(1)	10.5269(8)
β (deg.)	102.451(1)	109.023(1)
V (Å^3)	1350.1(2)	557.83(8)
Z	4	4
T (°C)	−80	20
λ (Å)	0.71073	0.71073
Maximum 2θ (deg.)	56.56	56.64
Observed data $I > 2\sigma(I)$	1584 (0.0302)	1334 (0.0237)
ρ_{calcd} (g cm^{-3})	4.456	4.262
μ(Mo$K\alpha$) (cm^{-1})	108.06	85.87
$R(F)$ for $F_o^2 > 2\sigma(F_o^2)^a$	0.0264	0.0273
$R_w(F_o^2)^b$	0.0891	0.0681

[a] $R(F) = \sum ||F_o| - |F_c|| / \sum |F_o|$.
[b] $R_w(F_o^2) = \left[\sum[w(F_o^2 - F_c^2)]^2 / \sum wF_o^2\right]^{1/2}$.

TABLE 2
Atomic Coordinates and Equivalent Isotropic Displacement Parameters for $K_2MoO_2(IO_3)_4$ (1)

Atom	x	y	z	U_{eq} (Å^2)^a
Mo(1)	0	0.1034(1)	$-\frac{1}{4}$	0.008(1)
I(1)	0.0344(1)	0.4154(1)	−0.4090(1)	0.009(1)
I(2)	0.2146(1)	0.5151(1)	−0.1800(1)	0.009(1)
K(1)	0.1859(1)	0.9996(2)	0.4637(1)	0.016(1)
O(1)	0.2782(4)	0.2749(8)	−0.1341(3)	0.020(1)
O(2)	−0.0200(3)	0.1738(7)	−0.3601(2)	0.012(1)
O(3)	0.1407(4)	0.5970(8)	−0.1090(3)	0.018(1)
O(4)	0.1530(3)	0.2770(7)	−0.4194(2)	0.014(1)
O(5)	−0.0547(3)	0.3257(7)	−0.4987(2)	0.011(1)
O(6)	0.1084(3)	0.3894(7)	−0.2534(2)	0.014(1)
O(7)	−0.1065(4)	−0.0712(7)	−0.2614(3)	0.014(1)

[a] U_{eq} is defined as one-third of the trace of the orthogonalized $\mathbf{U}_{ij}$ tensor.

TABLE 3
Atomic Coordinates and Equivalent Isotropic Displacement Parameters for β-$KMoO_3(IO_3)$ (2)

Atom	x	y	z	U_{eq} (Å^2)^a
Mo(1)	−0.2308(1)	0.0032(1)	0.2803(1)	0.010(1)
I(1)	−0.6446(1)	−0.1729(1)	0.0467(1)	0.012(1)
K(1)	−0.3436(1)	0.2329(1)	0.5732(1)	0.023(1)
O(1)	−0.5194(4)	0.0309(4)	0.1311(3)	0.014(1)
O(2)	−0.7843(5)	−0.2150(5)	0.1506(3)	0.022(1)
O(3)	−0.8207(4)	−0.0503(4)	−0.0879(3)	0.013(1)
O(4)	−0.2776(4)	−0.2544(4)	0.1979(3)	0.014(1)
O(5)	0.0012(4)	−0.0496(4)	0.3577(3)	0.017(1)
O(6)	−0.3342(4)	−0.0616(4)	0.3993(3)	0.015(1)

[a] U_{eq} is defined as one-third of the trace of the orthogonalized $\mathbf{U}_{ij}$ tensor.

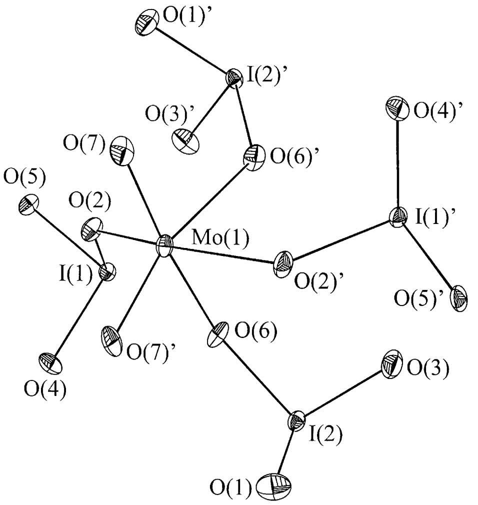

FIG. 1. A depiction of the discrete $[MoO_2(IO_3)_4]^{2-}$ anions found in $K_2[MoO_2(IO_3)_4]$ (**1**). Each molybdenum atom resides on a two-fold special position. Fifty percent probability ellipsoids are shown. The K^+ cations (not shown) separate the anions and form long ionic contacts with the terminal and bridging oxygen atoms of the iodate anions.

leads us to believe that some quantity of molybdenum stays in solution thus lowering the isolated yield of these compounds. When the mother liquor is left to evaporate, a white, non-crystalline powder is deposited. EDX analysis confirms the presence of Mo in these samples.

Structures

$K_2MoO_2(IO_3)_4$ (1). The structure of **1** is zero-dimensional or molecular and consists of $[MoO_2(IO_3)_4]^{2-}$ anions, shown in Fig. 1, separated by potassium cations. The Mo(VI) centers are ligated by two *cis* oxo ligands and four monodentate iodate anions. The two *cis* oxo ligands of compound **1** form a molybdenyl unit, MoO_2^{2+}, which has two short Mo=O bonds with an O=Mo=O bond angle of 103.6(3)°. The distorted octahedral geometry of the Mo atoms is described by a 2+2+2 pattern, where there are two short, two intermediate, and two long bonds (32). There are only three independent Mo–O bond lengths of 1.711(4), 1.957(4), and 2.235(4) Å present in **1** as a result of the Mo atom residing on a two-fold site. The shortest of these are with the terminal oxygen atoms of the molybdenyl group, while the intermediate and long bonds are with the bridging iodate anions. This bonding scheme is readily explained by an orthorhombic, second-order Jahn–Teller distortion along a C_2-axis of the MoO_6 octahedron (21, 22). Mo(VI) is readily susceptible to such distortions, because while the ground state (HOMO) has octahedral symmetry there is a low-lying excited state (LUMO) close enough in energy to allow for mixing (21, 22). Further-

TABLE 4
Selected Bond Distances (Å) and Angles (deg) for $K_2MoO_2(IO_3)_4$ (1)

Distances (Å)			
Mo(1)–O(7)	1.711(4)	Mo(1)–O(7)′	1.711(4)
Mo(1)–O(2)	1.957(4)	Mo(1)–O(2)′	1.957(4)
Mo(1)–O(6)	2.235(4)	Mo(1)–O(6)′	2.235(4)
I(1)–O(2)	1.909(4)	I(1)–O(4)	1.788(4)
I(1)–O(5)	1.829(4)	I(2)–O(1)	1.778(5)
I(2)–O(3)	1.803(5)	I(2)–O(6)	1.837(4)
Angles (deg)			
O(7)–Mo(1)–O(7)′	103.6(3)	O(7)–Mo(1)–O(2)′	100.5(2)
O(7)′–Mo(1)–O(2)′	95.0(2)	O(7)–Mo(1)–O(2)	95.0(2)
O(7)′–Mo(1)–O(2)	100.5(2)	O(2)′–Mo(1)–O(2)	154.8(2)
O(7)–Mo(1)–O(6)	165.3(2)	O(7)′–Mo(1)–O(6)	89.5(2)
O(2)′–Mo(1)–O(6)	84.8(2)	O(2)–Mo(1)–O(6)	75.7(2)
O(7)–Mo(1)–O(6)′	89.5(2)	O(7)′–Mo(1)–O(6)′	165.3(2)
O(2)′–Mo(1)–O(6)′	75.7(2)	O(2)–Mo(1)–O(6)′	84.8(2)
O(6)–Mo(1)–O(6)′	78.4(2)		

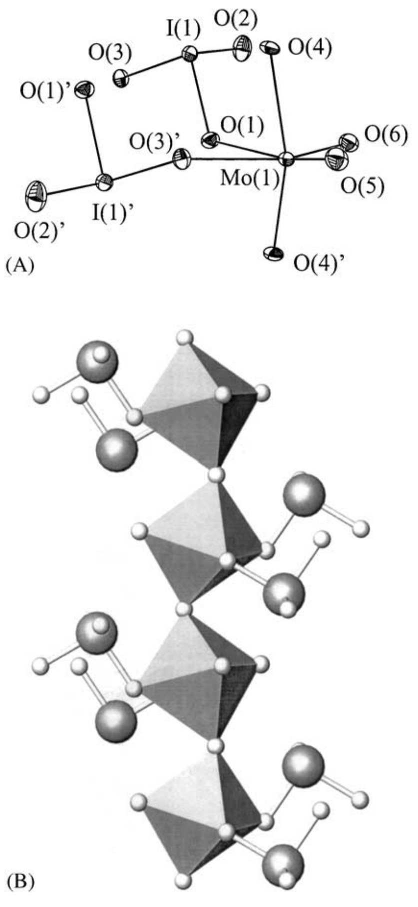

FIG. 2. (a) A view of the $[MoO_2O_{2/2}(IO_3)_{2/2}]$ structural building unit found in β-$KMoO_3(IO_3)$ (**2**). Fifty percent probability ellipsoids are shown. (b) Part of a molybdenyl iodate chain found in **2**. In these chains, the orientation of the molybdenyl units alternate as chain propagation occurs.

more, because the HOMO–LUMO gap decreases in size with increasing charge on the metal center, metal ions capable of obtaining high oxidation states, such as Mo(VI), tend to show particularly pronounced distortions (21, 22, 33). This type of distortion has also been noted in other Mo(VI) compounds including Mo(VI) selenites (32, 34, 35). In compound **1**, the Mo center is displaced by 0.37 Å from the center of the idealized MoO_6 octahedron.

I–O bond lengths are comparable to those found in AMoO$_3$(IO$_3$) (A = α,β-K, Rb, Cs) (28). The terminal I–O lengths are somewhat shorter ranging from 1.778(5) to 1.829(4) Å, while the bridging oxygen atoms contain longer I–O distances of 1.909(4) Å and 1.837(4) Å for $I(1)$ and $I(2)$, respectively. One crystallographically unique K^+ cation, two per formula unit, serves to balance charge in the compound. Both terminal and bridging oxygen atoms of the iodate anions form long ionic contacts with the eight-coordinate K^+ cations with interactions ranging from 2.711(4) to 3.249(5) Å. This creates an environment around the K^+ cations that is best described as an irregular dodecahedron. The bond valence sum for the molybdenum atom in **1** has a value of 5.78 which is in reasonable agreement with Mo(VI) (36). Additional bond lengths and angles for **1** are given in Table 4.

β-KMoO$_3$(IO$_3$) (2). The structure of **2** contains a similar type of bonding scheme for the molybdenum center as described for $K_2MoO_2(IO_3)_4$ (**1**). Although, in addition to the two terminal oxo groups, the distorted MoO_6 octahedra are completed by two oxygen atoms that bridge to adjacent octahedra, and two oxygen atoms from bridging iodate anions that form $[MoO_2O_{2/2}(IO_3)_{2/2}]$ structural building units (Fig. 2a). The Mo–O–Mo bridges establish one-dimensional chains of corner-sharing molybdenum octahedra extending along the b-axis. The previously reported α-KMoO$_3$(IO$_3$) phase, which is also two-dimensional, contains a key difference from **2** that is found in the molybdenum oxygen chain configurations. In α-KMoO$_3$(IO$_3$), the molybdenyl units are all aligned on the same side of a given chain. However, the molybdenyl moieties in β-KMoO$_3$(IO$_3$) (**2**) rotate as chain propagation occurs, as shown in Fig. 2b. This type of alternating chain configuration is found in the polar compounds AMoO$_3$(IO$_3$) (A = Rb, Cs) (28). Bridging iodate groups serve to stitch these chains into slabs creating an overall two-dimensional network shown in Fig. 3. Each molybdenum chain has only two neighboring chains, which are connected together by iodate groups. On a given molybdenum atom, the two bridged iodates are both connected to only one other molybdenum center on an adjacent chain to form an eight-membered ring. This results in more planar layers than the corrugated layers in α-KMoO$_3$(IO$_3$). The anionic slabs in **2** are separated by K^+ cations located in nine-coordinate, tricapped trigonal prismatic environments. The bond valence sum calculated for the molybdenum atom in **2** is 5.77 (36).

Based on I–O bond lengths found in several previously synthesized molybdenyl iodates (28), β-KMoO$_3$(IO$_3$) does not show any surprising contrasts. As expected, I–O bond lengths for oxygen atoms bound to a molybdenum center are longer than I–O bond lengths found for terminal oxygen atoms. The sole terminal iodate-bound oxygen atom has an I–O bond length of 1.773(3) Å while the two oxygen atoms bound to metal centers in the bridging iodate

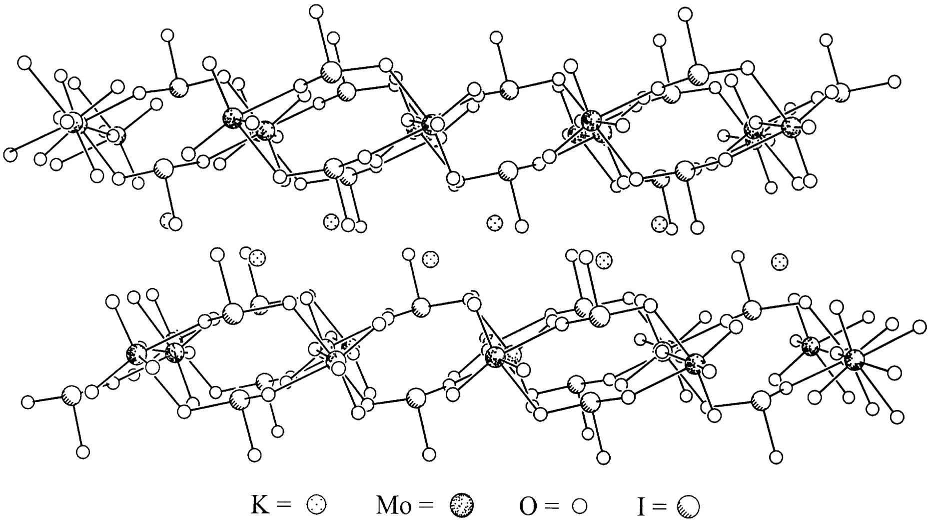

FIG. 3. An illustration of the two-dimensional structure of β-KMoO$_3$(IO$_3$) (**2**). On a given molybdenum atom, the two bridging iodate anions are both connected to only one other molybdenum center on an adjacent chain to form an eight-membered ring. The layers are separated by K^+ cations that form long ionic contacts with oxygen atoms from the iodate and molybdenyl groups.

TABLE 5
Selected Bond Distances (Å) and Angles (°) for β-$KMoO_3(IO_3)$ (2)

Distances (Å)			
Mo(1)–O(1)	2.231(3)	Mo(1)–O(3)′	2.210(3)
Mo(1)–O(4)	2.093(3)	Mo(1)–O(4)′	1.825(3)
Mo(1)–O(5)	1.709(3)	Mo(1)–O(6)	1.743(3)
I(1)–O(1)	1.857(3)	I(1)–O(2)	1.773(3)
I(1)–O(3)	1.836(3)		
Angles (°)			
O(3)′–Mo(1)–O(1)	76.1(1)	O(4)′–Mo(1)–O(4)	163.60(5)
O(4)–Mo(1)–O(3)′	79.8(1)	O(4) –Mo(1)–O(1)	78.5(1)
O(4)′–Mo(1)–O(3)′	87.0(1)	O(4)′–Mo(1)–O(1)	89.0(1)
O(5)–Mo(1)–O(6)	102.5(1)	O(5)–Mo(1)–O(3)′	91.1(1)
O(5)–Mo(1)–O(1)	163.8(1)	O(5)–Mo(1)–O(4)′	100.4(1)
O(5)–Mo(1)–O(4)	89.6(1)	O(6)–Mo(1)–O(4)′	101.0(1)
O(6)–Mo(1)–O(4)	89.3(1)	O(6)–Mo(1)–O(3)′	162.6(1)
O(6)–Mo(1)–O(1)	88.5(1)		

have I–O bond lengths of 1.836(3) and 1.857(3) Å. Additional bond lengths and angles for **2** can be found in Table 5.

CONCLUSIONS

In our report on the syntheses, structures, and properties of $AMoO_3(IO_3)$ (A = K, Rb, Cs), we postulated that there were two features that were responsible for the formation of polar structures with Rb^+ and Cs^+ cations and a centrosymmetric structure with K^+ cations (28). The first of these is the orientation of the molybdenyl, MoO_2^{2+}, units with respect to one another. For $RbMoO_3(IO_3)$ and $CsMoO_3(IO_3)$, these moieties alternate their orientation during chain translation. In α-$KMoO_3(IO_3)$, these groups are all oriented on the same side of the molybdenum oxide chain. This difference is one factor responsible for both the changes in dimensionality and polarity. However, in β-$KMoO_3(IO_3)$, we find the same type of molybdenyl iodate chain as in $RbMoO_3(IO_3)$ and $CsMoO_3(IO_3)$, and yet β-$KMoO_3(IO_3)$ is still layered like α-$KMoO_3(IO_3)$ and is likewise, centrosymmetric. This indicates that the alkali metal cations also play a key role in determining the structures of these compounds. In a similar example, when the Rb^+, Cs^+, and NH_4^+ cations are replaced with K^+ in the syntheses of $A[(VO)_2(IO_3)_3O_2]$ (A = Rb, Cs, NH_4), a different compound is obtained, and a change to a centrosymmetric crystal setting is also observed (37).

Finally, the observation that NH_4^+ cations do not become incorporated into the products of the reactions described herein is consistent with the cation selectivity that we observed in reactions involving both K^+ and Cs^+. When MoO_3 is reacted under hydrothermal conditions with IO_4^- in the presence of Cs^+ and K^+, only the Cs^+-containing product, $CsMoO_3(IO_3)$, was isolated. Based on the similarity in size between the Cs^+ and NH_4^+ cations, we would have predicted that $NH_4MoO_3(IO_3)$ would have been isolated from these reactions, but this was not the case. $NH_4MoO_3(IO_3)$ can however be prepared from the hydrothermal reaction of NH_4IO_4 with MoO_3.

ACKNOWLEDGMENTS

The authors express their gratitude to Auburn University, NASA (ASGC), and the Department of Energy, Heavy Elements Program (Grant DE-FG02-01ER15187) for support of this work.

REFERENCES

1. C. W. Blomstrand, *Z. Anorg. Chem.* **1,** 10 (1892).
2. M. P. Chrétien, *Ann. Chim. Phys. (Paris)* **15,** 358 (1898).
3. A. Rosenheim and O. Liebknecht, *Liebigs Ann. Chem.* **308,** 40 (1899).
4. C. Svenson, S. C. Abrahams, and J. L. Bernstein, *J. Solid State Chem.* **36,** 195 (1981).
5. K. Nassau, J. W. Shiever, and B. E. Prescott, *J. Solid State Chem.* **7,** 186 (1973).
6. K. Nassau, J. W. Shiever, and B. E. Prescott, *J. Solid State Chem.* **8,** 260 (1973).
7. K. Nassau, J. W. Shiever, B. E. Prescott, and A.S. Cooper, *J. Solid State Chem.* **11,** 314 (1974).
8. R. Liminga, S. C. Abrahams, and J. L. Bernstein, *J. Chem. Phys.* **62,** 755 (1975).
9. K. Nassau, J. W. Shiever, and B. E. Prescott, *J. Solid State Chem.* **14,** 122 (1975).
10. S. C. Abrahams, J. L. Bernstein, and K. Nassau, *J. Solid State Chem.* **16,** 173 (1976).
11. S. C. Abrahams, J. L. Bernstein, and K. Nassau, *J. Solid State Chem.* **22,** 243 (1977).
12. R. Liminga, S. C. Abrahams, and J. L. Bernstein, *J. Chem. Phys.* **67,** 1015 (1977).
13. P. K. S. Gupta, H. L. Ammon, and S. C. Abrahams, *Acta Crystallogr. C* **45,** 175 (1989).
14. J. G. Bergman Jr., G. D. Boyd, A. Ashkin, and S. K. Kurtz, *J. Appl. Phys.* **70,** 2860 (1969).
15. U. Opik and M. H. L. Pryce, *Proc. R. Soc. (London) A* **161,** 220 (1937).
16. R. A. Wheeler, M. H. Whangbo, T. Hughbanks, R. Hoffman, J. K. Burdett, and T. A. Albright, *J. Am. Chem. Soc.* **108,** 2222 (1986).
17. R. G. Pearson, *J. Mol. Struct.* **103,** 25 (1983).
18. S. K. Kang, H. Tang, and T. A. Albright, *J. Am. Chem. Soc.* **115,** 1971 (1993).
19. R. E. Cohen, *Nature* **358,** 136 (1992).
20. J. K. Burdett, "Molecular Shapes." Wiley-Interscience, New York, 1980.
21. M. Kunz and I. D. Brown, *J. Solid State Chem.* **115,** 395 (1995).
22. J.B. Goodenough and J. M. Longo, Crystallographic and magnetic properties of perovskite and perovskite-related compounds. In *Landolt-Bornstein* (Hellwege, K. H. and Hellwege, A. M. Eds.), Vol. 4, pp. 126–314 Springer-Verlag, Berlin, 1970.
23. I. D. Brown, *Acta Crystallogr. B* **33,** 1305 (1977).
24. P. Lofgren, *Acta Chem. Scand.* **21,** 2781 (1967).
25. W. Meschede, and R. Mattes, *Z. Anorg. Allg. Chem.* **420,** 25 (1976).
26. J. A. Ibers, and D. T. Cromer, *Acta. Crystallogr.* **11,** 794 (1958).

27. A. C. Bean, S. M. Peper, and T. E. Albrecht-Schmitt, *Chem. Mater.* **13,** 1266 (2001).
28. R. E. Sykora, K. M. Ok, P. S. Halasyamani, and T. E. Albrecht-Schmitt, *J. Am. Chem. Soc.* **124,** 1951 (2002).
29. R. H. Blessing, SADABS, Program for absorption correction using SMART CCD based on the method of Blessing. *Acta. Crystallogr. A* **51,** 33 (1995).
30. G. M. Sheldrick, "SHELXTL PC, Version 5.0, An Integrated System for Solving, Refining, and Displaying Crystal Structures from Diffraction Data." Siemens Analytical X-ray Instruments, Inc., Madison, WI, 1994.
31. A. L. Spek, *Acta Crystallogr. A* **46,** C34 (1990).
32. W. T. A. Harrison, L. L. Dussack, and A. J. Jacobson, *J. Solid State Chem.* **125,** 234 (1996).
33. P. S. Halasyamani, and K. R. Poeppelmeier, *Chem. Mater.* **10,** 2753 (1998).
34. W. T. A. Harrison, L. L. Dussack, and A. J. Jacobson, *Inorg. Chem.* **33,** 6043 (1994).
35. L. L. Dussack, W. T. A. Harrison, and A. J. Jacobson, *Mater. Res. Bull.* **31,** 249 (1996).
36. N. E. Brese, and M. O'Keeffe, *Acta Crystallogr. B* **47,** 192 (1991).
37. R. E. Sykora, K. M. Ok, P. S. Halasyamani, D. W. Wells, and T. E. Albrecht-Schmitt, *Chem. Mater.* (2002), in press.